Ryanodine receptor interaction with the SNARE-associated protein snapin

Spyros Zissimopoulos[1,*], Duncan J. West[2], Alan J. Williams[2] and F. Anthony Lai[1]

[1]Wales Heart Research Institute, Department of Cardiology, Cardiff University School of Medicine, Heath Park, Cardiff, CF14 4XN, UK
[2]Department of Cardiac Medicine, NHLI, Imperial College London, Dovehouse Street, London, SW3 6LY, UK
*Author for correspondence (e-mail: ZissimopoulosS@cardiff.ac.uk)

Accepted 14 February 2006
Journal of Cell Science 119, 2386-2397 Published by The Company of Biologists 2006
doi:10.1242/jcs.02936

Summary

The ryanodine receptor (RyR) is a widely expressed intracellular calcium (Ca^{2+})-release channel regulating processes such as muscle contraction and neurotransmission. Snapin, a ubiquitously expressed SNARE-associated protein, has been implicated in neurotransmission. Here, we report the identification of snapin as a novel RyR2-interacting protein. Snapin binds to a 170-residue predicted ryanodine receptor cytosolic loop (RyR2 residues 4596-4765), containing a hydrophobic segment required for snapin interaction. Ryanodine receptor binding of snapin is not isoform specific and is conserved in homologous RyR1 and RyR3 fragments. Consistent with peptide fragment studies, snapin interacts with the native ryanodine receptor from skeletal muscle, heart and brain. The snapin-RyR1 association appears to sensitise the channel to Ca^{2+} activation in [^{3}H]ryanodine-binding studies. Deletion analysis indicates that the ryanodine receptor interacts with the snapin C-terminus, the same region as the SNAP25-binding site. Competition experiments with native ryanodine receptor and SNAP25 suggest that these two proteins share an overlapping binding site on snapin. Thus, regulation of the association between ryanodine receptor and snapin might constitute part of the elusive molecular mechanism by which ryanodine-sensitive Ca^{2+} stores modulate neurosecretion.

Key words: Ryanodine receptor, Snapin, SNARE complex, Protein interaction, Neurosecretion

Introduction

Ionised calcium (Ca^{2+}) is the trigger for synaptic vesicle fusion with the presynaptic membrane and subsequent neurotransmitter release (Augustine et al., 2003; Neher, 1998). The trigger Ca^{2+} is provided by the extracellular fluid upon invasion of axon terminals by an action potential. Plasma membrane depolarisation activates voltage-gated Ca^{2+} channels leading to a transient local elevation of intracellular Ca^{2+} (up to 100 μM) in the presynaptic terminal active zone. Beside action-potential-evoked exocytosis, there is a vesicular release process not triggered by the depolarisation of the presynaptic nerve terminal (Bouron, 2001). This electrical-activity-independent release is called 'spontaneous' because the mechanisms triggering and controlling it are not known. Recently, presynaptic ryanodine-sensitive Ca^{2+} stores have been implicated in spontaneous, as well as depolarisation-induced, exocytosis in the central and peripheral nervous system.

The ryanodine receptor Ca^{2+}-release channel (RyR) is a large-conductance, cation-selective channel expressed in both excitable and non-excitable cells (Fill and Copello, 2002; Williams et al., 2001; George et al., 2005). Three mammalian RyR isoforms encoded by distinct genes have been purified, and their amino acid sequence deduced by cDNA cloning indicates ~70% identity. RyR1 is highly enriched in skeletal muscle but is also expressed in other tissues including some parts of the brain, most prominently in Purkinje cells of the cerebellum. RyR2 is the predominant form in cardiac muscle and is also the most widely and abundantly distributed isoform in the brain, and RyR3 has been found at low levels in several tissues. The RyR is primarily located on the sarcoplasmic reticulum (SR) of muscle cells and the endoplasmic reticulum (ER) of non-muscle cells, but is also found in mitochondria (Beutner et al., 2001) and secretory vesicles (Mitchell et al., 2001). Importantly, immunohistochemical methods have demonstrated the presence of RyRs in presynaptic boutons of hippocampal neurons (Sharp et al., 1993), chicken cerebellar granule and mossy fibre neurons (Ouyang et al., 1997), rat cerebellar basket cells (Llano et al., 2000), mouse hypothalamic neurons (De Crescenzo et al., 2004), differentiated NG108-15 neuronal cells (Ronde et al., 2000) and salamander photoreceptor inner segments (Krizaj et al., 2003). In addition, [^{3}H]ryanodine-binding sites have been shown in microsomal (ER), synaptosomal and subsynaptosomal fractions from rat hippocampus, cerebellum, cortex and spinal cord (Padua et al., 1996; Padua et al., 1991).

The presence of functional, ryanodine-sensitive presynaptic Ca^{2+} stores is demonstrated by the occurrence of fundamental Ca^{2+}-release events similar to those observed in heart and skeletal muscle ('Ca^{2+} sparks'). Such spontaneous localised Ca^{2+} transients have been reported in the presynaptic terminals of the lizard neuromuscular junction (Melamed-Book et al., 1999), rat cerebellar basket cells (Conti et al., 2004; Llano et al., 2000), rat hippocampal CA3 pyramidal cells (Emptage et al., 2001) and mouse hypothalamic neurons (De Crescenzo et al., 2004). Moreover, in the presynaptic terminals of cerebellar basket cells, the amplitude of the Ca^{2+} transient resulting from spontaneous Ca^{2+} release was comparable with that produced

by single action potentials (Conti et al., 2004). It has been suggested that these spontaneous Ca^{2+}-release events underlie the electrical-activity-independent, spontaneous transmitter release, at least in the synapses between cerebellar basket-Purkinje cells (Bardo et al., 2002; Llano et al., 2000) and hippocampal CA3 pyramidal neurons (Emptage et al., 2001; Savic and Sciancalepore, 1998).

RyR-mediated Ca^{2+}-induced Ca^{2+} release (CICR) triggered by depolarisation-induced Ca^{2+} entry, which contributes up to ~50% of the resulting elevation in intracellular Ca^{2+} concentration, has been demonstrated in presynaptic terminals in a variety of synapses, including the neuromuscular junction of the mouse and frog (Narita et al., 2000; Narita et al., 1998; Nishimura et al., 1990), bullfrog sympathetic ganglia (Cao and Peng, 1999; Peng, 1996), guinea-pig postganglionic sympathetic neurons (Smith and Cunnane, 1996), *Aplysia* buccal ganglion (Mothet et al., 1998), rat cerebellar basket cells (Galante and Marty, 2003; Llano et al., 2000), rat hippocampal CA3 pyramidal neurons (Emptage et al., 2001), rat mossy fibre neurons (Liang et al., 2002), rat barrel cortex layer II neurons (Simkus and Stricker, 2002), the NG108-15 neuronal cell line (Ronde et al., 2000), hair cells of the mouse and frog (Kennedy and Meech, 2002; Lelli et al., 2003) and salamander photoreceptor inner segments (Krizaj et al., 1999; Krizaj et al., 2003). Where studied, CICR was found to facilitate depolarisation-induced neurotransmitter release. The CICR mechanism and the resulting enhancement in neurotransmitter release might also be activated by Ca^{2+} originating from sources other than voltage-gated Ca^{2+} channels, in particular Ca^{2+} entry through presynaptic ionotropic nicotinic acetylcholine receptors (Brain et al., 2001; Sharma and Vijayaraghavan, 2003) or Ca^{2+} release from inositol (1,4,5)-trisphosphate [Ins(1,4,5)P_3]-sensitive Ca^{2+} stores following activation of presynaptic group I metabotropic glutamate receptors (Cochilla and Alford, 1998; Simkus and Stricker, 2002).

The SNARE (soluble *N*-ethylmaleimide-sensitive fusion protein attachment protein receptor) family of proteins have been implicated as the conserved core protein machinery for all intracellular membrane fusion events from yeast to humans (Chen and Scheller, 2001; Jahn et al., 2003). Three proteins of the presynaptic terminal – the plasma membrane proteins syntaxin and SNAP25 (25 kDa synaptosome-associated protein), and the synaptic vesicle protein VAMP (vesicle-associated membrane protein, also known as synaptobrevin) – were the first SNAREs to be identified. More than 100 other SNARE proteins from diverse organisms have been discovered to date. On the basis of sequence homology and domain structure, mammalian SNAREs have been categorised as members of the syntaxin, SNAP25 or VAMP families. Most of them are found in specific cellular compartments, suggesting that they have selective functional involvement in specific intracellular trafficking steps. Syntaxin, SNAP25 and VAMP assemble with a 1:1:1 stoichiometry into a ternary complex mediated by their cytoplasmic coiled-coil domains. Assembly of the SNARE core complex is believed to be the minimal requirement for initiation of the lipid fusion reaction.

Membrane fusion is regulated by several accessory proteins that bind to individual SNAREs and/or the assembled complex. One such protein is snapin, a small protein of 15 kDa that was originally described as neuron specific and located on synaptic vesicle membranes (Ilardi et al., 1999). Snapin interacts with the assembled SNARE core complex as well as with isolated SNAP25 through its C-terminal coiled-coil domain. Introduction of snapin peptides containing the SNAP25-binding sequence into cultured superior cervical ganglion neurons resulted in partial inhibition of synaptic transmission (by ~30%) (Ilardi et al., 1999). It was further shown that snapin is phosphorylated by cAMP-dependent protein kinase A (PKA) at Ser50, which enhanced its interaction with SNAP25 (Chheda et al., 2001). Over-expression of a serine to aspartic acid (S50D) snapin mutant (mimicking the phosphorylated state) in adrenal chromaffin cells resulted in a marked increase in secretion kinetics, indicating an increase in the number of release-competent, large dense-core vesicles (Chheda et al., 2001); by contrast, in cultured hippocampal neurons, the S50D mutant resulted in a reduced readily releasable vesicle pool with a concomitant increase in the probability of neurotransmitter release (Thakur et al., 2004). These studies have implicated snapin as a synapse-specific PKA target with an important regulatory role in neurotransmitter release. However, a recent study has challenged this idea, since snapin over-expression failed to influence any of the analysed parameters of neurotransmitter release in cultured hippocampal neurons (Vites et al., 2004), which was in agreement with results obtained (with wild-type snapin) from an independent group (Thakur et al., 2004). In addition, snapin was shown to have a broad tissue distribution and a predominantly cytoplasmic localisation (Buxton et al., 2003; Vites et al., 2004), and biochemical evidence indicated that snapin also interacts with SNAP23 (a ubiquitously expressed SNAP25-related protein), suggesting that snapin might have a general role in SNARE-mediated fusion events (Buxton et al., 2003). Evidence for a snapin role in intracellular membrane trafficking is provided by three recent reports. First, snapin was shown to interact with EBAG9 (estrogen-receptor-binding fragment-associated gene 9), which resulted in inhibition of regulated exocytosis of large dense-core vesicles in neurosecretory PC12 cells (Ruder et al., 2005). Second, snapin was found to interact with the vanilloid receptor and is involved in its plasma membrane incorporation from donor vesicles induced by activation of protein kinase C (Morenilla-Palao et al., 2004). Third, snapin was also found to interact with several subunits of BLOC-1 (biogenesis of lysosome-related organelles complex-1), which is involved in the biogenesis of specialised organelles of the endosomal-lysosomal system (Starcevic and Dell'Angelica, 2004). Additional interaction partners for snapin have been reported [regulator of G protein signalling 7 (Hunt et al., 2003), adenylyl cyclase type VI (Chou et al., 2004), TPR/MET tyrosine kinase (Schaaf et al., 2005)] with a function seemingly unrelated to membrane fusion.

As part of a study to identify novel RyR-associated proteins, we performed a yeast two-hybrid (Y2H) genetic screen and isolated snapin as an interacting partner for a RyR2 C-terminal fragment. The snapin-binding site is conserved in all three mammalian RyR isoforms, and snapin interaction with native RyR from skeletal and cardiac heavy SR as well as from brain synaptosomes was demonstrated. The RyR-binding region was mapped to the snapin C-terminus, the same location as the SNAP25 site. Competition binding experiments demonstrated that the native RyR and recombinant SNAP25 compete for snapin binding. Moreover, [^{3}H]ryanodine-binding assays

suggested that snapin increases the Ca^{2+} sensitivity of RyR1 channel activation. Our results indicate that mammalian RyRs interact with snapin in an association that might be involved in membrane fusion events and/or local intracellular Ca^{2+} signalling.

Results

Snapin interacts with the RyR C-terminus

Upon completion of a Y2H interaction screen of an adult cardiac muscle cDNA library with bait comprising a RyR2 C-terminal fragment (BT1B2, residues 4596-4765), a single positive clone was isolated, characterised and identified as snapin, from the public nucleotide sequence databases. The original interacting clone contained both 5′ and 3′ untranslated regions that were removed to generate (SnpAD), containing only the snapin coding sequence. A strong interaction was detected when BT1B2 and SnpAD were re-introduced into yeast (Fig. 1C), confirming that the positive association of RyR2 occurred specifically through snapin.

Importantly, no other RyR2 construct of a series of overlapping fragments spanning the entire 15 kb coding sequence of RyR2 scored for an interaction with SnpAD (not shown), demonstrating the RyR2 C-terminal domain specificity of the snapin association. We also examined whether the RyR2 C-terminal domain binds to SNAP25, a synaptic protein that contains coiled-coil domains homologous to those found in snapin. SNAP25AD failed to interact with BT1B2, as well as the panel of RyR2 overlapping fragments (not shown). The BT1B2-SnpAD interaction was further examined by swapping around the GAL4 DNA-BD and AD fusion partners; however, this failed to exhibit an interaction between SnpBT and AD1B2. Such directionality of interactions is not uncommon in the Y2H system, as we have previously observed this phenomenon for the transforming growth factor β receptor type I and FKBP12 pair (Zissimopoulos and Lai, 2005a), and it has also been observed in the case of snapin and BLOC-1 subunits (Starcevic and Dell'Angelica, 2004). This might be a result of the snapin conformation being altered when fused to the GAL4 DNA-BD, since the SnpBT construct displayed only weak binding with SNAP25AD, whereas a very strong interaction was detected in the SNAP25BT-SnpAD configuration (not shown, but see Fig. 3B).

According to one transmembrane topology model for RyR (Takeshima et al., 1989), BT1B2 encodes a single predicted cytosolic loop, although it also encompasses a distinct stretch of hydrophobic residues (amino acids 4718-4750). However, in another model of RyR topology, this hydrophobic segment is proposed to form a putative transmembrane (M7) domain (Zorzato et al., 1990). To localise further the snapin-binding site within BT1B2, we generated three overlapping sub-fragments (Fig. 1A). We found that BT1B, which lacks the putative transmembrane M7 domain was negative; by contrast, BT1B3, containing the whole of M7 and lacking the M7-M8 loop, was positive. BT1B4, encoding M7 and the M7-M8 loop, was negative for an interaction with snapin (Fig. 1C). These results suggest that the M7 hydrophobic segment of RyR2 is necessary, but not sufficient, for snapin binding.

The BT1B2-snapin interaction was further investigated using co-immunoprecipitation (co-IP) assays of proteins synthesised in vitro. Snapin is expressed as a single band in the cell-free TNT expression system, whereas BT1B2 appears as a triplet (irrespective of the presence of pancreatic microsomes). IP of BT1B2 with Ab^{Myc} was found to co-precipitate snapin, but only when the proteins

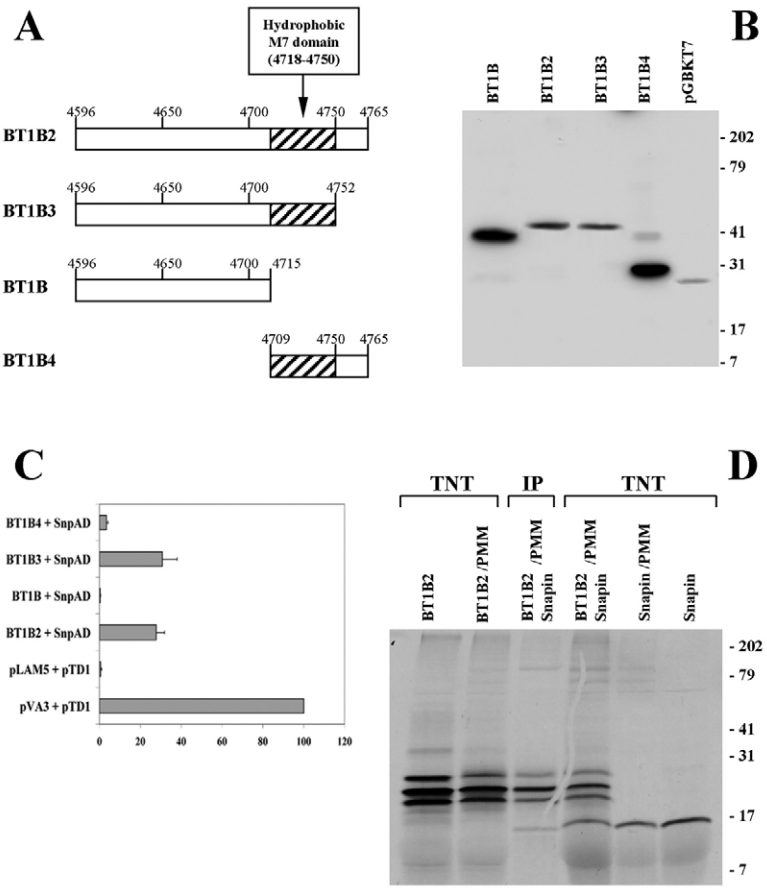

Fig. 1. Snapin interaction with the BT1B2 fragment of RyR2. (A) Schematic diagram of BT1B2 sub-overlapping fragments. (B) Protein expression of RyR2 fragments in yeast: protein extracts (50 μg per sample) of yeast Y190 transformed with plasmids as indicated were analysed by western blotting using Ab^{Myc} (12% SDS-PAGE gel; pGBKT7: empty vector). (C) Yeast two-hybrid liquid β-galactosidase assay of yeast Y190 transformed with the plasmids as indicated. Mean values of β-galactosidase units obtained from five individual colonies per sample, with normalisation against the positive control pVA3 + pTD1, are shown (pLAM5 + pTD1, negative control). (D) Snapin was tested for an interaction with BT1B2 using co-immunoprecipitation (IP) assays of proteins synthesised and radiolabelled in vitro. BT1B2 and snapin were co-expressed in the TNT system in the presence of canine pancreatic microsomal membranes (PMM), BT1B2 was immunoprecipitated by Ab^{Myc}, and the presence of co-precipitated snapin was analysed by autoradiography (15% SDS-PAGE gel). An aliquot of the TNT reaction (10% of the volume processed in co-IP) was included in the autoradiogram, as well as individual TNT reactions for BT1B2 and snapin to serve as molecular weight standards.

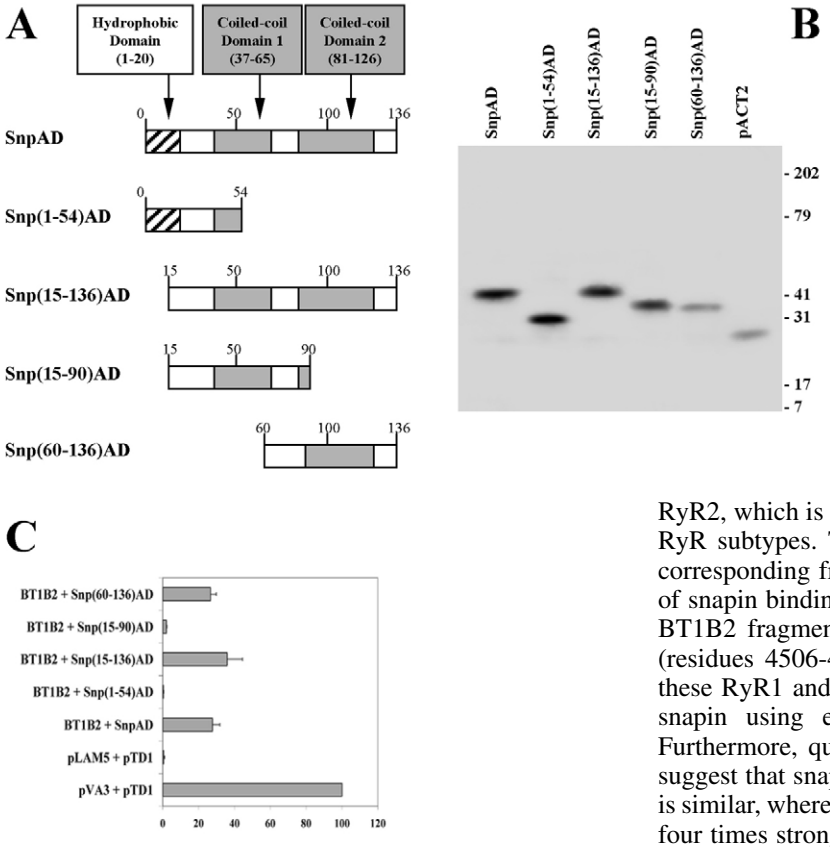

Fig. 2. Mapping the RyR2-interacting region of snapin. (A) Schematic diagram of snapin sub-overlapping fragments. (B) Protein expression of snapin fragments in yeast: protein extracts (50 μg per sample) of yeast Y190 transformed with plasmids as indicated were analysed by western blotting using Ab^{HA} (12% SDS-PAGE gel; pACT2: empty vector). (C) Yeast two-hybrid liquid β-galactosidase assay of yeast Y190 transformed with the plasmids as indicated. Mean values of β-galactosidase units obtained from five individual colonies per sample, with normalisation against the positive control, are shown.

were co-expressed in the presence of pancreatic microsomal membranes (Fig. 1D). No interaction was observed when the two proteins were expressed in the absence of pancreatic microsomes (not shown), suggesting that the hydrophobic M7 region requires a membrane environment for snapin association to occur.

RyR interacts with the snapin C-terminus

Snapin contains a short hydrophobic sequence at the extreme N-terminal – a putative transmembrane segment (Ilardi et al., 1999) – and two coiled-coil structures at the central and C-terminal domain (Buxton et al., 2003), with the C-terminal coiled-coil structure mediating the interaction with SNAP25 and SNAP23 (Buxton et al., 2003; Ilardi et al., 1999). To localise further the RyR2-binding site within snapin, we generated four overlapping snapin sub-fragments (Fig. 2A) and tested them for an interaction with BT1B2 in the Y2H system. We observed that BT1B2 was unable to interact with the N-terminal fragment of snapin (residues 1-54), whereas binding was retained with the truncated construct Snp(15-136)AD lacking the N-terminal hydrophobic domain (Fig. 2C). The association with RyR2 was also preserved with the most C-terminal fragment (residues 60-136), but not with the Snp(15-90)AD construct lacking the last third of snapin. We also confirmed that SNAP25 interacts with snapin and with Snp(60-136)AD in particular (not shown). These data indicate that the RyR2-interaction site is contained within coiled-coil domain at the C-terminus of snapin, overlapping with the SNAP25 site.

RyR isoforms bind to snapin

The BT1B2 fragment lies within the C-terminal region of RyR2, which is highly conserved among the three mammalian RyR subtypes. Thus, it is relevant to determine whether the corresponding fragments of RyR1 and RyR3 are also capable of snapin binding. Therefore, we generated the corresponding BT1B2 fragments of RyR1 (residues 4669-4834) and RyR3 (residues 4506-4669) in the same vector as for RyR2. Both these RyR1 and RyR3 constructs were found to interact with snapin using either the Y2H or co-IP assays (Fig. 3). Furthermore, quantitative liquid β-galactosidase Y2H assays suggest that snapin binding to each of the three RyR isoforms is similar, whereas snapin binding to SNAP25 is approximately four times stronger.

Association of snapin with native RyR

The above results suggest that an association between RyR and snapin might occur in vivo. To address this possibility, we generated two affinity-purified snapin antibodies raised to specific peptide antigens (snapin residues 98-111 and 122-136). However, an immunoreactive 15 kDa protein band was not detectable in rat brain, rabbit skeletal muscle or pig heart subcellular fractions, although a parallel positive control with recombinant purified snapin was detected (not shown). We attempted to detect RyR-snapin association in brain, skeletal muscle or heart homogenates despite the apparently low abundance of snapin and/or low antibody titre, but were unable to identify a 15 kDa endogenous snapin band after co-IP by RyR antibodies, even after lengthy exposure using enhanced chemiluminescence (ECL).

Thus, we examined whether the native RyR protein in skeletal muscle or cardiac heavy SR vesicles, or brain synaptosomes, interacts with recombinant snapin using co-IP assays. RyR immunoisolated from solubilised membrane fractions was incubated with [^{35}S]snapin synthesised in vitro, and evidence for RyR-bound snapin was analysed by autoradiography. As shown in Fig. 4, co-IP of [^{35}S]snapin was reproducibly observed with various RyR antibodies tested in all three tissues, suggesting snapin interacts with the distinct native RyR isoforms expressed in different tissues. We estimate that, under our co-IP conditions, <1% of the [^{35}S]snapin applied is recovered in the RyR immunoprecipitate. With cardiac SR, snapin recovery was higher for Ab^{1093} than Ab^{33}, as the former antibody is a potent immunoprecipitating reagent (Zissimopoulos and Lai, 2005b). Similarly, Ab^{2142} was more efficient than Ab^{33} in skeletal muscle SR. The lowest recovery

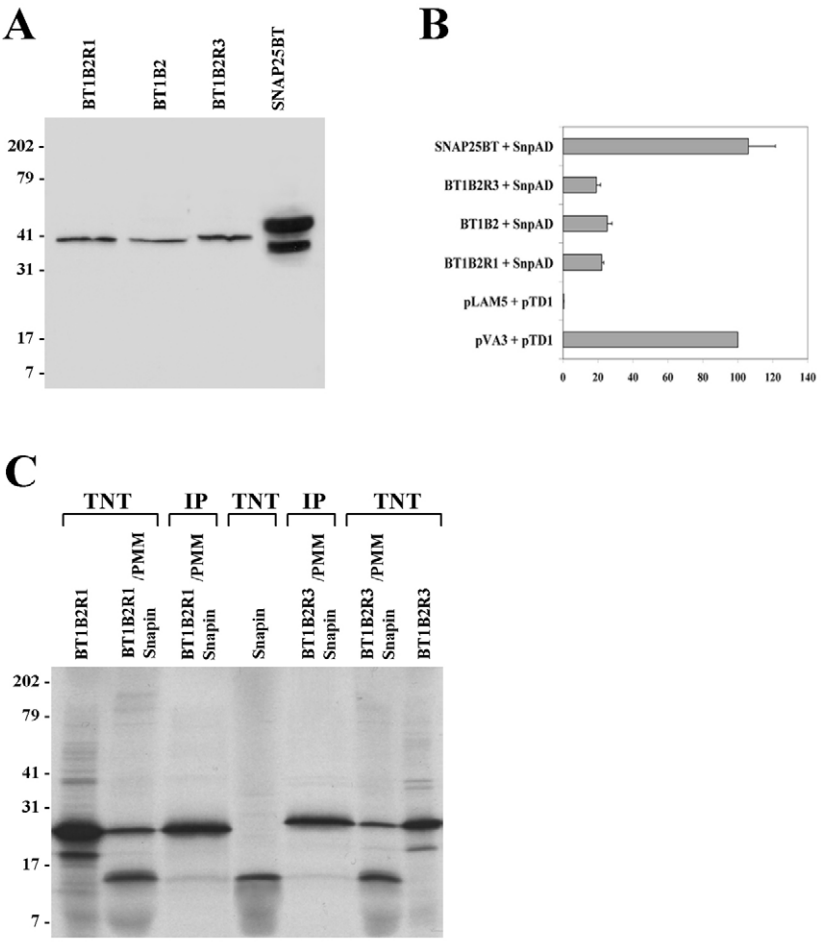

Fig. 3. Snapin interaction with the BT1B2 fragment of RyR1 and RyR3. (A) Protein expression of the corresponding BT1B2 fragments from the three mammalian RyRs and SNAP25 in yeast: protein extracts (50 μg per sample) of yeast Y190 transformed with plasmids as indicated were analysed by western blotting using Ab^{Myc} (12% SDS-PAGE gel). (B) Yeast two-hybrid liquid β-galactosidase assay of yeast Y190 transformed with the plasmids as indicated. Mean values of β-galactosidase units obtained from five individual colonies per sample, with normalisation against the positive control, are shown. (C) Snapin was tested for an interaction with the corresponding BT1B2 fragment of RyR1 and RyR3 using co-immunoprecipitation (IP) assays of proteins synthesised and radiolabelled in vitro. BT1B2R1/R3 and snapin were co-expressed in the TNT system in the presence of canine pancreatic microsomal membranes (PMM), the RyR fragment was immunoprecipitated by Ab^{Myc}, and the presence of co-precipitated snapin was analysed by autoradiography (15% SDS-PAGE gel). An aliquot of the TNT reaction (10% of the volume processed in co-IP) was included in the autoradiogram, as well as individual TNT reactions for BT1B2R1/R3 and snapin.

of snapin was observed for synaptosomes, owing to the decreased RyR expression levels relative to skeletal and cardiac muscle SR. Interestingly, although both Ab^{2142} (RyR1 specific) and Ab^{1093} (RyR2 specific) resulted in snapin co-IP with synaptosomes, recovery of snapin was highest for Ab^{33} (RyR consensus), suggesting that both RyR1 and RyR2 isoforms are expressed in rat brain synaptosomes.

Snapin interaction with native RyR from skeletal and cardiac heavy SR was also examined by glutathione *S* transferase (GST) affinity chromatography ('GST pull-down' assay). GST fused to the N-terminus of a snapin construct (GST-ΔNSnp) that contains the RyR-interacting region (residues 15-136, see Fig. 2C) was used to avoid potential expression problems associated with the N-terminal hydrophobic domain. GST-FKBP12.6 was used in parallel assays to serve as positive control, since FKBP12.6 interaction with both skeletal and cardiac RyR is very strong and well documented (Qi et al., 1998; Timerman et al., 1996). GST and GST-SNAP25 were employed as negative controls since our Y2H data showed no interaction of SNAP25 with RyR2 fragments. Incubation of solubilised SR vesicles with GST-ΔNSnp resulted in recovery of both RyR1 from skeletal and RyR2 from cardiac SR (Fig. 5). Importantly, no RyR was recovered by GST only or GST-SNAP25, demonstrating the specificity of the GST pull-down assay for RyR-snapin binding. The amount of RyR bound to GST-ΔNSnp was significantly less than to GST-FKBP12.6, suggesting that the RyR-snapin interaction is weaker than RyR-FKBP12.6.

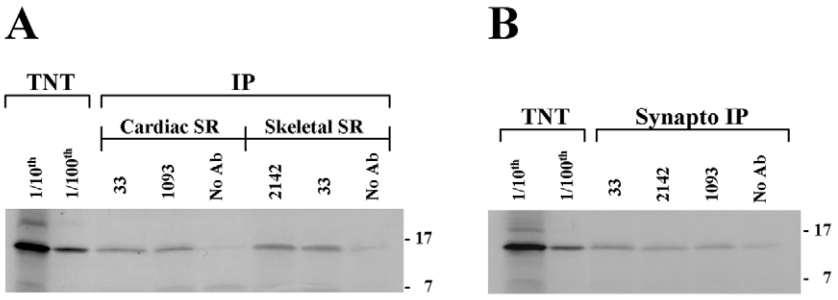

Fig. 4. Co-immunoprecipitation of native RyR with snapin. Native RyR was first immunoprecipitated (IP) with an appropriate antibody from solubilised (A) cardiac (2 mg) or skeletal muscle heavy SR (200 μg), or (B) synaptosomes (2 mg), and was subsequently incubated with radiolabelled, TNT-expressed snapin. Co-precipitated snapin was then analysed by autoradiography (15% SDS-PAGE gels). The first two lanes, showing 10% and 1% respectively, of the TNT reaction processed in the co-IPs provide a molecular weight standard and also enable estimation of co-immunoprecipitated snapin.

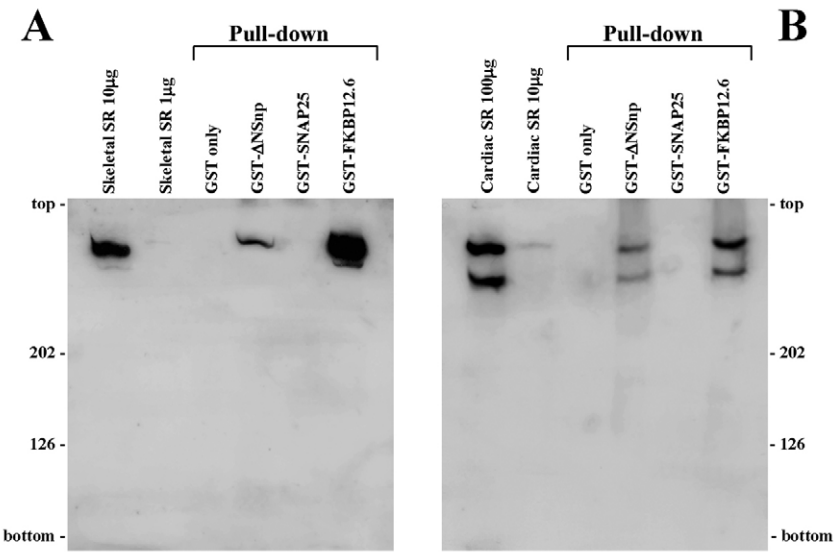

Fig. 5. GST affinity chromatography of snapin with native RyR. GST pull-down experiments of native RyR incubated with purified GST fusion proteins and detection by western blotting. Solubilised (A) skeletal muscle (200 µg) or (B) cardiac heavy SR (1 mg) were incubated with purified GST fusion proteins (2 nmol) as indicated, proteins were precipitated with glutathione-Sepharose 4B beads, and co-precipitated RyR was analysed by western blotting using Ab^{2149} (4% SDS-PAGE/agarose gels). The first two lanes show loading of (A) skeletal muscle or (B) cardiac heavy SR.

Snapin alters RyR function

The functional impact of snapin on the RyR Ca^{2+}-release channel was assessed by [^{3}H]ryanodine-binding assays. Ryanodine binding is widely used as a monitor of channel activity because high-affinity ryanodine binding (~10 nM K_d) occurs preferentially to the open state of the channel (Sutko et al., 1997). We investigated binding of [^{3}H]ryanodine to skeletal muscle RyR over a range of free Ca^{2+} concentrations in the presence or absence of snapin (purified GST-ΔNSnp, 1 µM). As shown in Fig. 6, a Ca^{2+}-dependent activation of ryanodine binding to RyR was obtained. [^{3}H]ryanodine binding was minimal in the virtual absence of Ca^{2+} [estimated $[Ca^{2+}]_{free}$ = 59 pM (West et al., 2002)], reflecting the closed state of the channel, whereas maximal binding was observed in the presence of 100 µM free Ca^{2+} and 1 mM ATP, conditions promoting a fully open channel. Notably, snapin enhanced [^{3}H]ryanodine binding to RyR1 at sub-micromolar free Ca^{2+} concentrations with a statistically significant effect at virtually zero free Ca^{2+} (44±5 fmol/mg in the presence of 1 µM GST-ΔNSnp compared with control 26±6 fmol/mg; a 69% increase) and also with 100 nM free Ca^{2+} (551±36 fmol/mg in the presence of 1 µM GST-ΔNSnp compared with control 363±11 fmol/mg; a 52% increase). These effects are entirely attributable to snapin since 1 µM GST had no significant effect in parallel experiments (32±12 fmol/mg at virtually zero free Ca^{2+}, 370±17 fmol/mg at 100 nM free Ca^{2+}). The stimulatory effect of snapin on ryanodine binding gradually diminished as the free Ca^{2+} concentration increased, and it was completely lost at high micromolar Ca^{2+} (Fig. 6). These results suggest that snapin sensitises the channel to Ca^{2+} activation of ryanodine binding, but does not affect maximal binding.

RyR and SNAP25 compete for snapin

Our Y2H data with snapin fragments suggest that the RyR2 BT1B2 fragment and SNAP25 share the same binding site on the snapin C-terminus (Fig. 2). This raises the possibility that in vivo the RyR and SNAP25 compete for snapin binding. To address this possibility, we performed competition binding experiments by using co-IP assays of native RyR with [^{35}S]snapin in the presence of increasing amounts of purified GST-SNAP25 (up to 1 µM). The total GST content was kept constant at 1 µM, made up with untagged GST, to avoid non-specific effects associated with the increasing amounts of protein added. RyR was first immunoprecipitated from solubilised skeletal muscle or cardiac heavy SR vesicles, and subsequently incubated with [^{35}S]snapin, synthesised in vitro, together with appropriate amounts of GST only and GST-SNAP25. Evidence for co-IP of [^{35}S]snapin with RyR was analysed by autoradiography. As shown in Fig. 7A and 7B, increasing amounts of SNAP25 resulted in reduced snapin recovery in RyR co-IPs from both skeletal muscle and heart

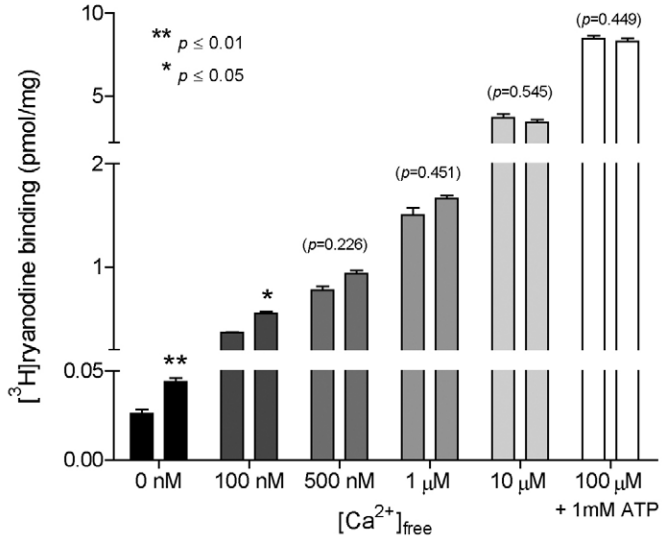

Fig. 6. Effect of snapin on [^{3}H]ryanodine binding to skeletal muscle RyR. Skeletal muscle heavy SR (50 µg) was incubated at a range of buffered free Ca^{2+} concentrations with 10 nM [^{3}H]ryanodine in the presence or absence of 1 µM GST-ΔNSnp. Non-specific binding was determined by the addition of 10 µM unlabelled ryanodine. A mean value of specific binding was determined from at least three separate experiments. For each Ca^{2+} concentration, the left column in the pair is the control and the right column is in the presence of snapin.

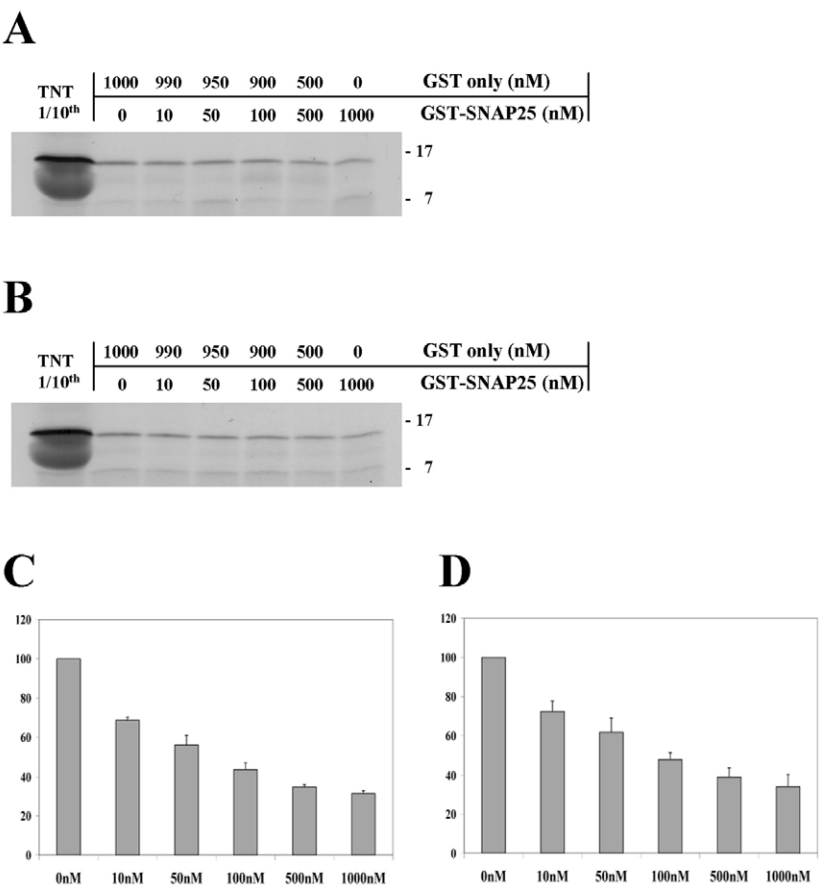

Fig. 7. SNAP25 and native RyR compete for snapin binding. Co-immunoprecipitation (co-IP) experiments of native RyR incubated with snapin radiolabelled and synthesised in vitro, in the presence of increasing amounts of SNAP25. RyR was first immunoprecipitated (A) with Ab^{2142} from solubilised skeletal muscle heavy SR (200 μg), or (B) with Ab^{1093} from solubilised cardiac heavy SR (2 mg), and subsequently incubated with radiolabelled, TNT-expressed snapin together with increasing amounts of purified GST-SNAP25 as indicated (total GST content constant to 1 μM made up with GST only), and co-precipitated snapin was analysed by autoradiography (15% SDS-PAGE gels). An aliquot of the TNT reaction, 10% of the volume processed in co-IP, was included in the first lane of the autoradiogram. Densitometry analysis was carried out from three separate experiments for (C) skeletal muscle or (D) cardiac heavy SR, followed by normalisation against the control sample (with no GST-SNAP25 but in the presence of 1 μM GST only).

SR. Densitometric analysis from several such experiments indicates that 1 μM of GST-SNAP25 (the highest concentration tested) results in about a threefold reduction in snapin association with RyR1 (31.6±1.4% of control) and RyR2 (34.3±6.1% of control), compared with control (no GST-SNAP25 plus 1 μM GST only) (Fig. 7C,D). These results suggest that SNAP25 and RyR compete for binding to the snapin C-terminus.

Discussion

The role of the intrinsic Ca^{2+}-release channel of the RyR in skeletal and cardiac muscle is to mediate rapid Ca^{2+} mobilisation from the SR store, thus providing the molecular trigger for skeletal muscle contraction and every heart beat. In the heart, cardiomyocyte contraction is initiated by massive Ca^{2+} release from RyR2. This release is gated by CICR mediated by Ca^{2+} entry through the L-type channel upon plasma membrane depolarisation. In skeletal muscle, activation of RyR1 occurs without Ca^{2+} entry as a result of a physical association with the L-type Ca^{2+} channel, although RyR1 is also amenable to CICR. The phenomenon of CICR, together with Ca^{2+} sparks, which is another subcellular physiological process known to be mediated by the RyR, have both been demonstrated in presynaptic terminals, and the contribution of internal ryanodine-sensitive Ca^{2+} stores in neurotransmitter release is now widely recognised (Bouchard et al., 2003; Verkhratsky, 2005).

In the present study, we identify snapin, a SNARE-associated protein, as an RyR2-interacting partner following a Y2H genetic screen of a cardiac muscle cDNA library (Fig. 1). Snapin was initially described as a neuron-specific protein (Ilardi et al., 1999), however recent studies using western blot as well as northern blot analyses have demonstrated that both the protein and transcript for snapin have a widespread expression, including the heart (Buxton et al., 2003; Vites et al., 2004). Using the complementary Y2H and co-IP assays, we have localised the snapin interaction with RyR2 to the C-terminal domain (BT1B2; Figs 2, 3). BT1B2 is located within the RyR transmembrane assembly, containing a long hydrophobic stretch of at least 30 residues that has been proposed to form a transmembrane segment (M7) by the 10TM model (Zorzato et al., 1990), but is absent from the 4TM model (Takeshima et al., 1989). More recent experimental evidence indicates that this long hydrophobic stretch forms a transmembrane helical hairpin that dips into the endo/sarcoplasmic reticulum membrane (Du et al., 2002). In this study, our deletion analysis suggests the presence of the RyR M7 domain is necessary, but not sufficient, for snapin binding (Fig. 2). However, BT1B2-snapin binding does not involve a direct interaction between both their hydrophobic domains, since specific binding was retained with truncated snapin constructs lacking the N-terminal hydrophobic segment. Thus, the hydrophobic RyR M7 domain appears to be required for BT1B2 to assume the correct conformation to enable snapin binding. This idea is fully consistent with the co-IP data, where RyR-snapin interaction is absent unless pancreatic microsomal membranes are included in the in vitro synthesis reaction,

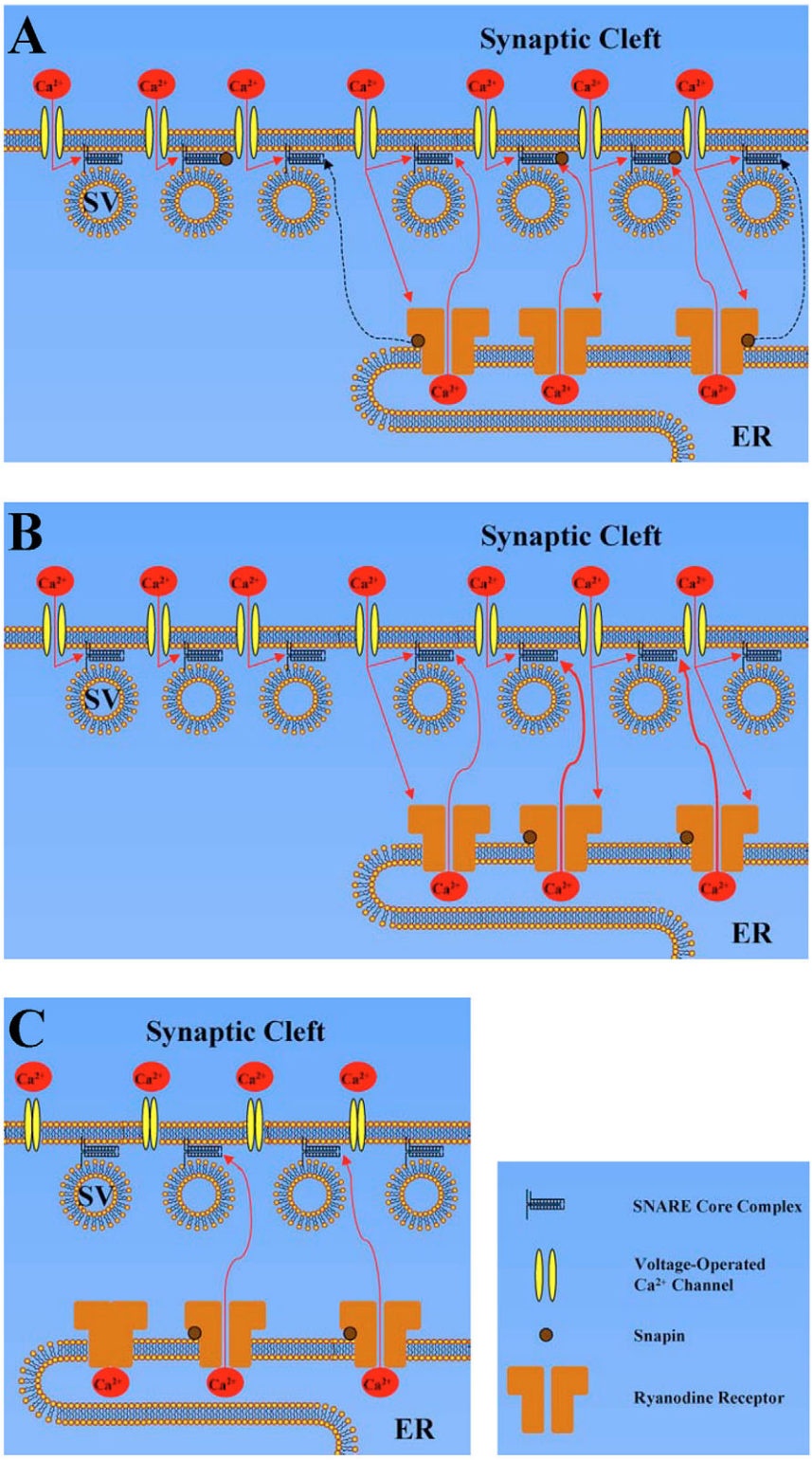

Fig. 8. Potential role for RyR and snapin in neurotransmitter release. (A) The arrival of an action potential at the presynaptic terminal causes plasma membrane depolarisation and Ca^{2+} entry through voltage-operated Ca^{2+} channels. Ca^{2+} entry induces fusion of synaptic vesicles (SV) with the plasma membrane through a process involving the SNARE core complex and synaptotagmin, and this process is reinforced through the interaction of snapin with SNAP25. In addition, Ca^{2+} entry activates RyR channels that are mobilising Ca^{2+} from internal stores. RyR channel activation and/or the rise in intracellular Ca^{2+} might cause snapin dissociation from the RyR and translocation to SNAP25, resulting in further enhancement of neurotransmitter release. (B) Ca^{2+} entry through voltage-operated Ca^{2+} channels induces fusion of synaptic vesicles with the plasma membrane and consequent neurotransmitter release. Furthermore, RyR channels located on the endoplasmic reticulum (ER) are activated by the Ca^{2+}-induced Ca^{2+}-release mechanism and provide an additional source of Ca^{2+}. Snapin interaction with the RyR might increase channel open probability and result in augmented Ca^{2+} release. (C) In the absence of plasma membrane depolarisation, some membrane fusion events still occur, most probably as a result of spontaneous localised Ca^{2+}-release events from ryanodine-sensitive Ca^{2+} stores. Snapin interaction with the RyR might increase Ca^{2+} spark frequency and/or amplitude, accounting for spontaneous neurotransmitter release.

suggesting the potential requirement for a transmembrane location of the M7 domain.

Our results using distinct RyR isoform peptide fragments also indicate that all three mammalian RyRs are capable of associating with snapin with qualitatively similar affinity (Fig. 3). An in vivo interaction between RyR and snapin was not demonstrated in this study. This might be explained by recent reports that demonstrate snapin, although ubiquitously expressed, occurs at very low levels (Buxton et al., 2003; Vites et al., 2004). Moreover, an interaction between endogenous snapin and SNAP23 was not demonstrated, although a strong interaction was shown by Y2H and in vitro binding assays (Buxton et al., 2003). The authors speculated that, inside the cell, the SNAP23-snapin interaction is a transient intermediate in the SNARE functional cycle and/or is inhibited by additional endogenous proteins. Similarly, the RyR-snapin interaction might be of transient nature or inhibited by additional endogenous proteins. However, our inability to identify an in vivo interaction between snapin and the RyR by co-IP assays might also be partly a result of the low affinity of our snapin antibodies, since standard western blot analysis did not reveal a 15 kDa protein band in various tissue subcellular fractions. Importantly, co-IP experiments with exogenous radiolabelled snapin, as well as GST pull-down assays, confirmed that the native RyR from skeletal muscle, heart and brain are capable of interaction with snapin (Figs 4, 5). This suggests that the RyR-snapin interaction might have a conserved role in a variety of cell types, since the three

mammalian RyRs and snapin have a widespread tissue expression.

At present, the physiological significance of the RyR-snapin association remains to be defined, but it might be involved in the mechanism of neurotransmitter release. Indeed, there is overwhelming evidence for the physical and functional presence of presynaptic RyRs and their modulatory role in neurotransmission (see Introduction). However, direct biochemical evidence that demonstrates explicit bridging of the processes of RyR-mediated Ca^{2+} release and SNARE-mediated membrane fusion is still pending. Snapin, a SNARE-associated protein with a facilitatory role in neurosecretion (Chheda et al., 2001; Ilardi et al., 1999; Ruder et al., 2005; Thakur et al., 2004) (but see Vites et al., 2004), could provide the elusive molecular link to regulation by the Ca^{2+} mobilised from internal stores. Specific insight into how snapin achieves this task may be assisted by our present finding that RyR and SNAP25 compete for snapin. Moreover, we have demonstrated that both the RyR- and SNAP25-interacting regions are located within the snapin C-terminal domain and, significantly, that SNAP25 is able to displace bound snapin from the native RyR (Fig. 7). It is plausible to speculate that translocation of snapin from the RyR to the SNARE complex depends on the level of cytosolic Ca^{2+}, RyR activation status and/or snapin phosphorylation status (Fig. 8A). Thus, it will be of interest to characterise the effect of Ca^{2+} and phosphorylation status on the RyR-snapin interaction in future studies. Alternatively, snapin binding to the RyR C-terminus and transmembrane assembly, and close to the channel pore, might exert a regulatory effect on channel function. Initial evidence of the functional effects of snapin association has been demonstrated by our [^{3}H]ryanodine-binding assays indicating that snapin increases the Ca^{2+} sensitivity of channel activation (Fig. 6). Hence, in resting cells, where the intracellular Ca^{2+} concentration is maintained in the low nanomolar range ($\leqslant$100 nM), RyR channels that are bound to snapin will be predicted to have an increased open probability that could be manifested by increased Ca^{2+} spark frequency and/or amplitude and by an increased sensitivity to CICR. This would in turn suggest that snapin association with RyR results in enhanced spontaneous, as well as depolarisation-induced, neurotransmitter release (Fig. 8B,C). Whatever is the precise mechanism, our current findings suggest that snapin and internal ryanodine-sensitive Ca^{2+} stores are interconnected and their role in neurotransmission should be investigated in parallel, an approach that could help explain the disparate results previously obtained in studies addressing the role of snapin.

The RyR-snapin association might not only be involved in neurotransmitter release but also in other Ca^{2+}-dependent membrane fusion reactions such as regulated exocytosis of secretory granules, since the required intracellular Ca^{2+} elevation could be a result of either Ca^{2+} entry across the plasma membrane or Ca^{2+} release from internal stores (Burgoyne and Morgan, 2003; Petersen et al., 1999). It is also noteworthy that, whereas regulated secretion has been traditionally regarded as a specialised process present only in a few cell types, recent studies have reported Ca^{2+}-regulated exocytosis of conventional lysosomes (Andrews, 2000; Gerasimenko et al., 2001) and a novel population of small vesicles distinct from known organelles (Borgonovo et al., 2003). Furthermore, certain intracellular fusion reactions, previously considered to be constitutive, are dependent on a final Ca^{2+}-triggering step (Burgoyne and Clague, 2003). Interestingly, Ca^{2+} efflux from the vesicular lumen has been shown to drive fusion between yeast vacuoles (Peters and Mayer, 1998), early endosomes (Holroyd et al., 1999), late endosomes with lysosomes (Pryor et al., 2000) and intra-Golgi cisternae (Porat and Elazar, 2000).

In conclusion, we have identified snapin as a novel RyR-interacting partner capable of altering its function and have demonstrated the competitive nature of its interaction with RyR and SNAP25. Further studies are required to elucidate how the RyR-snapin association regulates the Ca^{2+}-release properties of the RyR channel and SNARE-mediated membrane fusion.

Materials and Methods

Antibodies

Ab^{Myc}, a mouse monoclonal anti-Myc antibody (9E10; Santa Cruz), was used at 1:500 dilution for western blotting and 1:50 dilution for immunoprecipitation (IP); Ab^{HA}, a rabbit polyclonal anti-haemaglutinin (HA) antibody (Y-11; Santa Cruz), was used at 1:500 dilution for western blotting. The RyR1-specific Ab^{2142} (epitope at 830-845 of RyR1) (Zissimopoulos and Lai, 2005a), RyR2-specific Ab^{1093} (epitope at 4454-4474 of RyR2), RyR consensus Ab^{33} (epitope at 2876-2896 of RyR2) and Ab^{2149} (epitope at 4933-4948 of RyR2) (Zissimopoulos and Lai, 2005b) were used at 1:500 dilution for western blotting and 1:20 dilution for IP. Snapin antibodies were custom generated from a commercial supplier (Eurogentec). Two synthetic peptides, ILQNAQERLRRLNH and AMLDSGVYPPGSPSK, which correspond to residues 98-111 and 122-136 of mouse snapin, were used to immunise rabbits, and snapin antibodies were affinity purified against each peptide.

Plasmid construction

The human RyR2 overlapping fragments (BT constructs) including BT1B and BT1B2 have been previously described (Stewart et al., 2003; Zissimopoulos and Lai, 2005a). BT1B3 [CAGCCCATGGTTATTTTTAAGCGAGAA forward (*Nco*I) and TACTGTCGACAAGATGGTTCATAATGT reverse (*Sal*I) with a built-in stop codon; underlined region indicates restriction enzyme recognition sequence] and BT1B4 [ATGTGGATCCTAGGAGTCGTTTTCACT forward (*Bam*HI) and GGTTAAGTCGACCTATTTGCCA reverse (*Sal*I) with a built-in stop codon] were generated by PCR amplification using a plasmid containing the full-length cDNA sequence of human RyR2, and cloned into the Y2H pGBKT7 vector (Clontech). The corresponding BT1B2 fragments of RyR1 and RyR3, designated BT1B2R1 [GGGGATCCTCAAGCGGGAGAA forward (*Bam*HI) and TCATCTCGAGCTATTTCCCATTGT reverse (*Xho*I) with a built-in stop codon] and BT1B2R3 [CACTCCATGGTATTCAAAAGGGAAAAA forward (*Nco*I) and TGGACTCGAGAACCAACTATTTGCCATT reverse (*Xho*I) with a built-in stop codon] respectively, were generated by PCR amplification using plasmids containing the full-length cDNA sequence of rabbit RyR1 or rabbit RyR3 and cloned into pGBKT7.

Full-length snapin without the 5′ and 3′ untranslated regions (UTRs) present in the clone isolated from the Y2H screen was generated by PCR amplification [TTCGCCATGGCGGGGGCTGGTTCC forward (*Nco*I) and AACAGTCGACTTATTTGCCTGGGGAGCCA reverse (*Sal*I)] using the original snapin clone as a template, and cloned into both the Y2H vectors to produce SnpBT and SnpAD constructs. Snp(15-136)AD [GCAGGGATCCCGGTGGCGGGG forward (*Bam*HI) and AACAGTCGACTTATTTGCCTGGGGAGCCA reverse (*Sal*I)] and Snp(60-136)AD [AATTGGATCCTAGCCACAGAACTGTGC forward (*Bam*HI) and AACAGTCGACTTATTTGCCTGGGGAGCCA reverse (*Sal*I)], were generated by PCR amplification using the original snapin clone as a template, and cloned into the Y2H pACT2 vector (Clontech). Snp(1-54)AD and Snp(15-90)AD were constructed by restriction digestion of SnpAD and Snp(15-136)AD respectively, using the endogenous *Sac*I-161 and *Mlu*I-270 (blunted with Pfu DNA polymerase) restriction sites, respectively at the 3′ cloning end. For in vitro expression of snapin, the full-length sequence was subcloned in the T7-containing vector pCR3 (Invitrogen). For expression of GST-ΔNSnp in bacteria, the cDNA insert from Snp(15-136)AD was subcloned in the pGEX-5X-2 vector (Amersham Pharmacia).

The cDNA encoding the entire length of human SNAP25 (β isoform, GenBank accession no. L19761) was generated by PCR amplification [GCTACCATGGCCGAAGACGCAGAC forward (*Nco*I) and ACGGGTCGACACACTTAACCACTTCCCAG reverse (*Sal*I)] from a human hippocampus cDNA library (Stratagene) and cloned into both the Y2H vectors. For expression of GST-SNAP25 in bacteria, the SNAP25 cDNA insert was subcloned into pGEX-5X-2. All constructs were verified by direct DNA sequencing (BigDye, Perkin-Elmer).

Yeast two-hybrid assay

The Y2H system was obtained from Clontech and all yeast handling, transformation and other Y2H techniques were performed according to the MatchMaker GAL4 User Manual and Yeast Protocols Handbook (Clontech). A human heart cDNA library (Clontech) was screened with BT1B2 using the CG1945 yeast strain. The screen of ~10^5 independent clones produced one interacting clone surviving on histidine-deficient medium (supplemented with 5 mM 3-amino-1,2,4-triazole) and having a positive blue phenotype in β-galactosidase assay. The interacting clone harboured a ~900 bp cDNA insert with an identical match to human snapin (GenBank accession no. AF086837) containing the entire coding sequence together with some 5′ UTR (encoding IRGRVDFV in-frame with the GAL4 AD) and the 3′ UTR. A trimmed version of snapin containing only the coding sequence was generated as described above. The Y190 strain was used in subsequent experiments and for the liquid β-galactosidase assays (o-nitrophenyl β-D-galactopyranoside as substrate). Protein expression in yeast was verified by western blotting.

Cell-free protein expression

In vitro cell-free protein expression was carried out using the TNT T7 Quick coupled transcription and translation system (Promega). Reactions were carried out in 10 μl volumes by adding 1 μg of plasmid DNA and 1 μl (0.53 MBq or 14 μCi) of [^{35}S]-labelled methionine (Pro-Mix, Amersham Biosciences) to the TNT mix. Where necessary, 1.5 μl of canine pancreatic microsomes (Promega) was included. For co-translation experiments, reactions were scaled up to 20 μl volume in the presence of the two plasmids (1 μg each) and 3 μl of canine pancreatic microsomes. Reaction samples were incubated in a 30°C water bath for 90 minutes, and terminated by placing on ice. The Y2H pGBKT7 vector, which contains the T7 promoter upstream of the Myc tag, results in expression of the recombinant protein fused to the Myc tag at the N-terminus, but not the GAL4 DNA-BD.

Preparation of GST fusion proteins

GST fusion proteins were expressed and purified from bacterial cultures according to the GST Gene Fusion System Handbook (Amersham Biosciences). Briefly, 500 ml of bacterial culture (*Escherichia coli* BL21; Novagen) carrying the appropriate expression plasmid was grown at 30°C. Protein expression was induced at 25°C by 0.1 mM isopropyl β-D-thiogalactoside when the optical density (at 600 nm) reached 0.5. Cells were harvested 3 hours later and the pellet was resuspended in 25 ml of PBS buffer (137 mM NaCl, 2.7 mM KCl, 10 mM Na_2HPO_4, 1.8 mM KH_2PO_4, pH 7.4) supplemented with 2 mg/ml of lysozyme and complete protease inhibitor cocktail (Roche), and incubated overnight at 4°C. Cells were permeabilised by a combination of freeze-thaw cycles (in liquid nitrogen) and brief sonication bursts, and the insoluble material was removed at 14,000 ***g*** for 10 minutes at 4°C. GST fusion proteins were isolated by incubation of the bacterial supernatant with glutathione-Sepharose 4B beads (1 ml bed volume, Amersham Biosciences) for 2 hours at 4°C with gentle mixing. Beads were washed twice with PBS containing 0.5% Triton X-100 and once with PBS. GST fusion proteins were eluted with 10 mM reduced glutathione (in 50 mM Tris-HCl, pH 8) following incubation for 30 minutes at 25°C. Reduced glutathione was removed with the use of a Vivaspin 20 concentrator (10,000 molecular weight cut-off; Vivascience) and the buffer was exchanged for PBS. Purified GST fusion proteins were stored at –80°C until use.

Preparation of tissue membrane fractions

Synaptosomes from rat whole brain (adult Wistar rats) were prepared using a discontinuous Percoll gradient centrifugation procedure according to Breukel et al. with some modifications (Breukel et al., 1997). Two freshly dissected rat brains were homogenized in 10 volumes of homogenisation buffer [0.32 M sucrose, 5 mM Hepes, 0.1 mM EDTA, pH 7.5, and complete protease inhibitor cocktail (Roche)] with the use of a Teflon-glass homogeniser, motor driven at 750 rpm (~10 strokes). Nuclei and unbroken cells were sedimented at ~1,500 ***g*** (2600 rpm, Beckman Allegra 6R) for 10 minutes at 4°C and the brain homogenate (diluted to 30 ml) was directly loaded on top of four Percoll gradients. Each gradient comprised three layers of 7.5% (12 ml), 10% (16 ml) and 23% (6 ml) Percoll in homogenisation buffer. The 7.5% top layer was prepared by mixing 7.5 ml of brain homogenate with 4.5 ml of 20% Percoll. The gradient was centrifuged at ~23,000 ***g*** (11,000 rpm, Beckman SW28.1 rotor) for 30 minutes at 4°C in a swing-out rotor (brake off), and synaptosomes were collected from the 10%-23% interface. Synaptosomes were diluted with storage buffer (132 mM NaCl, 3 mM KCl, 2 mM $MgSO_4$, 1.2 mM NaH_2PO_4, 0.02 mM $CaCl_2$, 10 mM Hepes, 10 mM glucose, pH 7.4), and Percoll was removed by centrifugation at ~200,000 ***g*** (40,000 rpm, Beckman 50.2Ti rotor) for 40 minutes at 4°C. Synaptosomes (sedimenting as a 'fluffy' layer on top of the Percoll pellet) were resuspended in storage buffer (with complete protease inhibitor cocktail) at 10 mg/ml protein concentration, and stored at –80°C. Skeletal muscle heavy SR from rabbit and cardiac heavy SR vesicles from pig hearts were prepared as described previously (Zissimopoulos and Lai, 2005b).

Co-immunoprecipitation assays

Proteins expressed in vitro were solubilised in 200 μl of IP buffer (20 mM Tris-HCl, 150 mM NaCl, 0.4% CHAPS, pH 7.4) by incubation for 1 hour at 4°C. Ab^{Myc} was added and the sample was incubated for 2 hours at 4°C with continuous mixing. Protein G Dynabeads (20 μl, Dynal) were added and the incubation continued for a further 2 hours. Protein immunocomplexes were isolated with the use of a magnetic particle concentrator (MPC-S, Dynal), and beads were washed three times with IP buffer. Immunoprecipitated proteins were resuspended in SDS-PAGE loading buffer (60 mM Tris, 2% SDS, 10% glycerol, 5 mM EDTA, 2% β-mercaptoethanol, 0.01% bromophenol blue, pH 6.8), heated at 85°C for 5 minutes, and analysed by SDS-PAGE and autoradiography.

For experiments with native RyR, skeletal muscle (200 μg) or cardiac heavy SR vesicles (2 mg), or synaptosomes (2 mg) were used. Membrane fractions were solubilised in 500 μl of IP buffer by overnight incubation at 4°C with continuous mixing, and the insoluble material was pelleted at 20,000 ***g*** for 10 minutes at 4°C. The RyR was immunoprecipitated by an appropriate antibody and Protein G Dynabeads following incubation for 6 hours at 4°C, resuspended in fresh 200 μl of IP buffer, and mixed overnight at 4°C with radiolabelled snapin synthesised in vitro. Immunoprecipitated proteins were washed three times with IP buffer and analysed by autoradiography. Where multiple snapin IP samples were processed, the individual TNT reactions were mixed and an equal aliquot was distributed to the IP samples, in order to minimise variations in protein expression.

GST pull-down assays

Skeletal muscle (200 μg) or cardiac heavy SR vesicles (1 mg) were solubilised in 200 μl of IP buffer by overnight incubation at 4°C with continuous mixing, and the insoluble material was pelleted at 20,000 ***g*** for 10 minutes at 4°C. Solubilised proteins were incubated overnight at 4°C with 2 nmol of a GST fusion protein (52 μg of GST only, 80 μg of GST-ΔNSnp, 100 μg of GST-SNAP25, 76 μg of GST-FKBP12.6) pre-captured on glutathione-sepharose 4B beads (30 μl bed volume; Amersham Biosciences). Beads were washed three times with IP buffer, and precipitated proteins were eluted with SDS-PAGE loading buffer and heating at 85°C for 5 minutes. Eluted proteins were separated on 4% SDS-PAGE gels strengthened with agarose, according to the method described by Tatsumi and Hattori (Tatsumi and Hattori, 1995), and analysed by western blotting using an RyR antibody.

Western blot analysis

Proteins from SDS-PAGE gels were transferred to a polyvinylidene difluoride membrane (Immobilon-P; Millipore) using a semi-dry transfer system (Trans-Blot SD; Bio-Rad) in transfer buffer (48 mM Tris, 39 mM glycine, 0.0375% SDS, 20% methanol) at 18 V for 1 hour. RyR was transferred at 20 V for 4 hours and methanol was omitted from the buffer. The membrane was blocked with 5% non-fat milk protein (Marvel) in TBS-T buffer (20 mM Tris, 137 mM NaCl, 0.1% Tween-20, pH 7.4). Primary antibodies were applied in the appropriate dilution overnight at 4°C, followed by horseradish peroxidase-linked secondary antibody (Santa Cruz). Immunoreactive protein bands were visualised by enhanced chemiluminescence detection (ECL; Amersham Biosciences).

Autoradiography

Radiolabelled proteins were separated by SDS-PAGE and the gel was fixed (40% methanol, 10% acetic acid) for 30 minutes. The fixing solution was removed and the gel was incubated with a fluorographic enhancer (Amplify; Amersham Biosciences) for a further 30 minutes and subsequently dried. The dried gel was exposed to an X-ray film (Kodak) at –80°C for variable periods of time. Densitometry analysis was performed using a GS-700 scanner (Bio-Rad) and Quantity One software (Bio-Rad).

[^{3}H]Ryanodine-binding analysis

Ryanodine binding was performed as previously described (West et al., 2002), using 10 nM [^{3}H]ryanodine (Amersham Pharmacia), 50 μg of skeletal muscle heavy SR and 1 μM GST-ΔNSnp or GST only as appropriate. Incubation was for 90 minutes at 37°C in a basic binding buffer (1 M KCl, 25 mM Pipes, pH 7.4) with buffered free Ca^{2+} (using 10 mM EGTA for zero Ca^{2+} or 1 mM NTA for all other concentrations). Free Ca^{2+} concentrations were calculated using MaxChelator software (http://www.stanford.edu/~cpatton/maxc.html). Non-specific binding was measured by co-incubation with 10 μM unlabelled ryanodine. Bound [^{3}H]ryanodine was separated from unbound by vacuum filtering through glass filters (Whatman GF/F). Radioactivity was quantified by liquid scintillation counting.

This research was supported by Wellcome Trust grant 066410 (F.A.L.) and by the BHF (A.J.W.). We thank C. George and L. Blayney for helpful discussions and excellent technical advice. We are grateful to P. Allen and Y. Hakamata for the RyR1 and RyR3 plasmids, respectively.

References

Andrews, N. (2000). Regulated secretion of conventional lysosomes. *Trends Cell Biol.* **10**, 316-321.

Augustine, G., Santamaria, F. and Tanaka, K. (2003). Local calcium signaling in neurons. *Neuron* **40**, 331-346.

Bardo, S., Robertson, B. and Stephens, G. (2002). Presynaptic internal Ca^{2+} stores contribute to inhibitory neurotransmitter release onto mouse cerebellar Purkinje cells. *Br. J. Pharmacol.* **137**, 529-537.

Beutner, G., Sharma, V., Giovannucci, D., Yule, D. and Sheu, S. (2001). Identification of a ryanodine receptor in rat heart mitochondria. *J. Biol. Chem.* **276**, 21482-21488.

Borgonovo, B., Cocucci, E., Racchetti, G., Podini, P., Bachi, A. and Meldolesi, J. (2003). Regulated exocytosis: a novel, widely expressed system. *Nat. Cell Biol.* **4**, 955-962.

Bouchard, R., Pattarini, R. and Geiger, J. (2003). Presence and functional significance of presynaptic ryanodine receptors. *Prog. Neurobiol.* **69**, 391-418.

Bouron, A. (2001). Modulation of spontaneous quantal release of neurotransmitters in the hippocampus. *Prog. Neurobiol.* **63**, 613-635.

Brain, K., Trout, S., Jackson, V., Dass, N. and Cunnane, T. (2001). Nicotine induces calcium spikes in single nerve terminal varicosities: a role for intracellular calcium stores. *Neuroscience* **106**, 395-403.

Breukel, A., Besselsen, E. and Ghijsen, W. (1997). Synaptosomes: a model system to study release of multiple classes of neurotransmitters. *Methods Mol. Biol.* **72**, 33-47.

Burgoyne, R. and Clague, M. (2003). Calcium and calmodulin in membrane fusion. *Biochim. Biophys. Acta* **1641**, 137-143.

Burgoyne, R. and Morgan, A. (2003). Secretory granule exocytosis. *Physiol. Rev.* **83**, 581-632.

Buxton, P., Zhang, X.-M., Walsh, B., Sriratana, A., Schenberg, I., Manickam, E. and Rowe, T. (2003). Identification and characterization of snapin as a ubiquitously expressed SNARE-binding protein that interacts with SNAP23 in non-neuronal cells. *Biochem. J.* **375**, 433-440.

Cao, Y. and Peng, Y. (1999). Caffeine and carbonyl cyanide m-chlorophenylhydrazone increased evoked and spontaneous release of luteinizing hormone-releasing hormone from intact presynaptic terminals. *Neuroscience* **92**, 1511-1521.

Chen, Y. and Scheller, R. (2001). SNARE-mediated membrane fusion. *Nat. Rev. Mol. Cell Biol.* **2**, 98-106.

Chheda, M., Ashery, U., Thakur, P., Rettig, J. and Sheng, Z.-H. (2001). Phosphorylation of snapin by PKA modulates its interaction with the SNARE complex. *Nat. Cell Biol.* **3**, 331-338.

Chou, J.-L., Huang, C.-L., Lai, H.-L., Hung, A., Chien, C.-L., Kao, Y.-Y. and Chern, Y. (2004). Regulation of type VI adenylyl cyclase by snapin, a SNAP25-binding protein. *J. Biol. Chem.* **279**, 46271-46279.

Cochilla, A. and Alford, S. (1998). Metabotropic glutamate receptor-mediated control of neurotransmitter release. *Neuron* **20**, 1007-1016.

Conti, R., Tan, Y. and Llano, I. (2004). Action potential-evoked and ryanodine-sensitive spontaneous Ca^{2+} transients at the presynaptic terminal of a developing CNS inhibitory synapse. *J. Neurosci.* **24**, 6946-6957.

De Crescenzo, V., ZhuGe, R., Velazquez-Marrero, C., Lifshitz, L., Custer, E., Carmichael, J., Lai, F., Tuft, R., Fogarty, K., Lemos, J. et al. (2004). Ca^{2+} syntillas, miniature Ca^{2+} release events in terminals of hypothalamic neurons, are increased in frequency by depolarization in the absence of Ca^{2+} influx. *J. Neurosci.* **24**, 1226-1235.

Du, G., Sandhu, B., Khanna, V., Guo, X. and MacLennan, D. (2002). Topology of the Ca^{2+} release channel of skeletal muscle sarcoplasmic reticulum (RyR1). *Proc. Natl. Acad. Sci. USA* **99**, 16725-16730.

Emptage, N., Reid, C. and Fine, A. (2001). Calcium stores in hippocampal synaptic boutons mediate short-term plasticity, store-operated Ca^{2+} entry, and spontaneous transmitter release. *Neuron* **29**, 197-208.

Fill, M. and Copello, J. (2002). Ryanodine receptors calcium release channels. *Physiol. Rev.* **82**, 893-922.

Galante, M. and Marty, A. (2003). Presynaptic ryanodine-sensitive calcium stores contribute to evoked neurotransmitter release at the basket cell-Purkinje cell synapse. *J. Neurosci.* **23**, 11229-11234.

George, C., Yin, C. and Lai, F. (2005). Toward a molecular understanding of the structure-function of ryanodine receptor Ca^{2+} release channels: perspectives from recombinant expression systems. *Cell Biochem. Biophys.* **42**, 197-222.

Gerasimenko, J., Gerasimenko, O. and Petersen, O. (2001). Membrane repair: Ca^{2+}-elicited lysosomal exocytosis. *Curr. Biol.* **11**, R971-R974.

Holroyd, C., Kistner, U., Annaert, W. and Jahn, R. (1999). Fusion of endosomes involved in synaptic vesicle recycling. *Mol. Biol. Cell* **10**, 3035-3044.

Hunt, R., Edris, W., Chanda, P., Nieuwenhuijsen, B. and Young, K. (2003). Snapin interacts with the N-terminus of regulator of G protein signaling 7. *Biochem. Biophys. Res. Commun.* **303**, 594-599.

Ilardi, J., Mochida, S. and Sheng, Z.-H. (1999). Snapin: a SNARE-associated protein implicated in synaptic transmission. *Nat. Neurosci.* **2**, 119-124.

Jahn, R., Lang, T. and Sudhof, T. (2003). Membrane fusion. *Cell* **112**, 519-533.

Kennedy, H. and Meech, R. (2002). Fast Ca^{2+} signals at mouse inner hair cell synapse: a role for Ca^{2+}-induced Ca^{2+} release. *J. Physiol.* **539**, 15-23.

Krizaj, D., Bao, J.-X., Schmitz, Y., Witkovsky, P. and Copenhagen, D. (1999). Caffeine-sensitive calcium stores regulate synaptic transmission from retinal rod photoreceptors. *J. Neurosci.* **19**, 7249-7261.

Krizaj, D., Lai, F. and Copenhagen, D. (2003). Ryanodine stores and calcium regulation in the inner segments of salamander rods and cones. *J. Physiol.* **547**, 761-774.

Lelli, A., Perin, P., Martini, M., Ciubotaru, C., Prigioni, I., Valli, P., Rossi, M. and Mammano, F. (2003). Presynaptic calcium stores modulate afferent release in vestibular hair cells. *J. Neurosci.* **23**, 6894-6903.

Liang, Y., Yuan, L.-L., Johnston, D. and Gray, R. (2002). Calcium signaling at single mossy fiber presynaptic terminals in the rat hippocampus. *J. Neurophysiol.* **87**, 1132-1137.

Llano, I., Gonzalez, J., Caputo, C., Lai, F., Blayney, L., Tan, Y. and Marty, A. (2000). Presynaptic calcium stores underlie large-amplitude miniature IPSCs and spontaneous calcium transients. *Nat. Neurosci.* **3**, 1256-1265.

Melamed-Book, N., Kachalsky, S., Kaiserman, I. and Rahamimoff, R. (1999). Neuronal calcium sparks and intracellular calcium "noise". *Proc. Natl. Acad. Sci. USA* **96**, 15217-15221.

Mitchell, K., Pinton, P., Varadi, A., Tacchetti, C., Ainscow, E., Pozzan, T., Rizzuto, R. and Rutter, G. (2001). Dense core secretory vesicles revealed as a dynamic Ca^{2+} store in neuroendocrine cells with a vesicle-associated membrane protein aequorin chimaera. *J. Cell Biol.* **155**, 41-51.

Morenilla-Palao, C., Planells-Cases, R., Garcia-Sanz, N. and Ferrer-Montiel, A. (2004). Regulated exocytosis contributes to protein kinase C potentiation of vanilloid receptor activity. *J. Biol. Chem.* **279**, 25665-25672.

Mothet, J.-P., Fossier, P., Meunier, F.-M., Stinnakre, J., Tauc, L. and Baux, G. (1998). Cyclic ADP-ribose and calcium-induced calcium release regulate neurotransmitter release at a cholinergic synapse of *Aplysia*. *J. Physiol.* **507**, 405-414.

Narita, K., Akita, T., Osanai, M., Shirasaki, T., Kijima, H. and Kuba, K. (1998). A Ca^{2+}-induced Ca^{2+} release mechanism involved in asynchronous exocytosis at frog motor nerve terminals. *J. Gen. Physiol.* **112**, 593-609.

Narita, K., Akita, T., Hachisuka, J., Huang, S.-M., Ochi, K. and Kuba, K. (2000). Functional coupling of Ca^{2+} channels to ryanodine receptors at presynaptic terminals: amplification of exocytosis and plasticity. *J. Gen. Physiol.* **115**, 519-532.

Neher, E. (1998). Vesicle pools and Ca^{2+} microdomains: new tools for understanding their roles in neurotransmitter release. *Neuron* **20**, 389-399.

Nishimura, M., Tsubaki, K., Yagasaki, O. and Ito, K. (1990). Ryanodine facilitates calcium-dependent release of transmitter at mouse neuromuscular junctions. *Br. J. Pharmacol.* **100**, 114-118.

Ouyang, Y., Martone, M., Deerinck, T., Airey, J., Sutko, J. and Ellisman, M. (1997). Differential distribution and subcellular localisation of ryanodine receptor isoforms in the chicken cerebellum during development. *Brain Res.* **775**, 52-62.

Padua, R., Wan, W., Nagy, J. and Geiger, J. (1991). [^{3}H]Ryanodine binding sites in rat brain demonstrated by membrane binding and autoradiography. *Brain Res.* **542**, 135-140.

Padua, R., Nagy, J. and Geiger, J. (1996). Subcellular localization of ryanodine receptors in rat brain. *Eur. J. Pharmacol.* **298**, 185-189.

Peng, Y.-Y. (1996). Ryanodine-sensitive component of calcium transients evoked by nerve firing at presynaptic nerve terminals. *J. Neurosci.* **16**, 6703-6712.

Peters, C. and Mayer, A. (1998). Ca^{2+}/calmodulin signals the completion of docking and triggers a late step of vacuole fusion. *Nature* **396**, 575-580.

Petersen, O., Burdakov, D. and Tepikin, A. (1999). Polarity in intracellular calcium signalling. *BioEssays* **21**, 851-860.

Porat, A. and Elazar, Z. (2000). Regulation of intra-Golgi membrane transport by calcium. *J. Biol. Chem.* **275**, 29233-29237.

Pryor, P., Mullock, B., Bright, N., Gray, S. and Luzio, J. (2000). The role of intraorganellar Ca^{2+} in late endosome-lysosome heterotypic fusion and in the reformation of lysosomes from hybrid organelles. *J. Cell Biol.* **149**, 1053-1062.

Qi, Y., Ogunbunmi, E., Freund, E., Timerman, A. and Fleischer, S. (1998). FK-binding protein is associated with the ryanodine receptor of skeletal muscle in vertebrate animals. *J. Biol. Chem.* **273**, 34813-34819.

Ronde, P., Dougherty, J. and Nichols, R. (2000). Functional IP_3- and ryanodine-sensitive calcium stores in presynaptic varicosities of NG108-15 (rodent neuroblastoma x glioma hybrid) cells. *J. Physiol.* **529**, 307-319.

Ruder, C., Riemer, T., Delgado-Martinez, I., Hermosilla, R., Engelsberg, A., Nehring, R., Dorken, B. and Rehm, A. (2005). EBAG9 adds a new layer of control on large dense-core vesicle exocytosis via interaction with snapin. *Mol. Biol. Cell* **16**, 1245-1257.

Savic, N. and Sciancalepore, M. (1998). Intracellular calcium stores modulate miniature GABA-mediated synaptic currents in neonatal rat hippocampal neurons. *Eur. J. Neurosci.* **10**, 3379-3386.

Schaaf, C., Benzing, J., Schmitt, T., Erz, D., Tewes, M., Bartram, C. and Janssen, J. (2005). Novel interaction partners of the TPR/MET tyrosine kinase. *FASEB J.* **19**, 267-269.

Sharma, G. and Vijayaraghavan, S. (2003). Modulation of presynaptic store calcium induces release of glutamate and postsynaptic firing. *Neuron* **38**, 929-939.

Sharp, A., McPherson, P., Dawson, T., Aoki, C., Campbell, K. and Snyder, S. (1993). Differential immunohistochemical localization of inositol 1,4,5-trisphosphate- and ryanodine-sensitive Ca^{2+} release channels in rat brain. *J. Neurosci.* **13**, 3051-3063.

Simkus, C. and Stricker, C. (2002). The contribution of intracellular calcium stores to mEPSCs recorded in layer II neurones of rat barrel cortex. *J. Physiol.* **545**, 521-535.

Smith, A. and Cunnane, T. (1996). Ryanodine-sensitive calcium stores involved in neurotransmitter release from sympathetic nerve terminals of the guinea-pig. *J. Physiol.* **497**, 657-664.

Starcevic, M. and Dell'Angelica, E. (2004). Identification of snapin and three novel proteins (BLOS1, BLOS2, and BLOS3/reduced pigmentation) as subunits of biogenesis of lysosome-related organelles complex-1 (BLOC-1). *J. Biol. Chem.* **279**, 28393-28401.

Stewart, R., Zissimopoulos, S. and Lai, F. (2003). Oligomerization of the cardiac ryanodine receptor C-terminal tail. *Biochem. J.* **376**, 795-799.

Sutko, J., Airey, J., Welch, W. and Ruest, L. (1997). The pharmacology of ryanodine and related compounds. *Pharmacol. Rev.* **49**, 53-98.

Takeshima, H., Nishimura, S., Matsumoto, T., Ishida, H., Kangawa, K., Minamino, N., Matsuo, H., Ueda, M., Hanaoka, M., Hirose, T. et al. (1989). Primary structure and expression from complementary DNA of skeletal muscle ryanodine receptor. *Nature* **339**, 439-445.

Tatsumi, R. and Hattori, A. (1995). Detection of giant myofibrillar proteins connectin and nebulin by electrophoresis in 2% polyacrylamide slab gels strengthened with agarose. *Anal. Biochem.* **224**, 28-31.

Thakur, P., Stevens, D., Sheng, Z.-H. and Rettig, J. (2004). Effects of PKA-mediated phosphorylation of snapin on synaptic transmission in cultured hippocampal neurons. *J. Neurosci.* **24**, 6476-6481.

Timerman, A., Onoue, H., Xin, H., Barg, S., Copello, J., Wiederrecht, G. and Fleischer, S. (1996). Selective binding of FKBP12.6 by the cardiac ryanodine receptor. *J. Biol. Chem.* **271**, 20385-20391.

Verkhratsky, A. (2005). Physiology and pathophysiology of the calcium store in the endoplasmic reticulum of neurons. *Physiol. Rev.* **85**, 201-279.

Vites, O., Rhee, J.-S., Schwarz, M., Rosenmund, C. and Jahn, R. (2004). Reinvestigation of the role of snapin in neurotransmitter release. *J. Biol. Chem.* **279**, 26251-26256.

West, D., Smith, E. and Williams, A. (2002). A novel and rapid approach to isolating functional ryanodine receptors. *Biochem Biophys. Res. Commun.* **294**, 402-407.

Williams, A., West, D. and Sitsapesan, R. (2001). Light at the end of the Ca^{2+}-release channel tunnel: structures and mechanisms involved in ion translocation in ryanodine receptor channels. *Q. Rev. Biophys.* **34**, 61-104.

Zissimopoulos, S. and Lai, F. (2005a). Central domain of the human cardiac muscle ryanodine receptor does not mediate interaction with FKBP12.6. *Cell Biochem. Biophys.* **43**, 203-220.

Zissimopoulos, S. and Lai, F. (2005b). Interaction of FKBP12.6 with the cardiac ryanodine receptor C-terminal domain. *J. Biol. Chem.* **280**, 5475-5485.

Zorzato, F., Fujii, J., Otsu, K., Phillips, M., Green, N., Lai, F., Meissner, G. and MacLennan, D. (1990). Molecular cloning of cDNA encoding human and rabbit forms of the Ca^{2+} release channel (ryanodine receptor) of skeletal muscle sarcoplasmic reticulum. *J. Biol. Chem.* **265**, 2244-2256.